

## FLUCTUATIONS AND THE QCD PHASE DIAGRAM

VOLKER KOCH

Nuclear Science Division, Lawrence Berkeley National Laboratory  
Berkeley, CA, 94720, USA

ADAM BZDAK

AGH University of Science and Technology  
Faculty of Physics and Applied Computer Science  
30-059 Kraków, Poland

*(Received June 7, 2016)*

*Dedicated to Andrzej Bialas in honour of his 80th birthday*

In this contribution, we will discuss how the study of various fluctuation observables may be used to explore the phase diagram of the strong interaction. We will briefly summarize the present study of experimental and theoretical research in this area. We will then discuss various corrections and issues which need to be understood and applied for a meaningful comparison of experimental measurements with theoretical predictions.

DOI:10.5506/APhysPolB.47.1867

## 1. Introduction

Soon after the discovery of QCD [1], and following the realization that QCD exhibits asymptotic freedom [2, 3], it was recognized that QCD predicts a new high temperature phase of weakly interacting quarks and gluons, termed the Quark–Gluon Plasma [4–6]. The existence of a new phase was confirmed in the first calculations using the lattice formulation of QCD, initially for pure SU(2) gauge theory [7, 8]. Over the years, as lattice QCD methods have been refined to allow for continuum extrapolated calculations with dynamical quarks at the physical masses, it has been found that the transition from hadrons to partons at vanishing net-baryon density is an analytic cross over [9]. At the same time, many model calculations suggested that at vanishing temperature but large baryon density, there might be a first-order transition [10]. This first-order phase transition will end at a

critical point, the location of which is not really constrained by any model calculations let alone lattice QCD, which, due to the fermion sign problem, can only explore regions of small net-baryon chemical potential,  $\mu_B/T \lesssim 1$ .

The potential presence of a first-order phase co-existence region together with a critical point has motivated a dedicated experimental program at RHIC, the so-called RHIC Beam Energy Scan (BES). Experimentally, regions of higher baryon density can be reached by lowering the beam energy where some of the projectile and target baryons are stopped at mid-rapidity. The study of fluctuations play an important role in the quest to experimentally explore the QCD phase diagram. Both, the second-order phase transition associated with a critical point and the first-order transition give rise to characteristic fluctuation pattern. Of course, the system produced in a heavy-ion collision is of finite size and evolves in time which smoothens the singular structures associated with phase transitions. However, fluctuation measurements are still helpful in this case, because, as we shall discuss below, fluctuations are related to derivatives of the free energy. For example, cumulants of the baryon number are given by derivatives with respect to the baryon chemical potential,  $\mu_B$ , *etc.* Therefore, the measurement of cumulants of a sufficient high order will allow to explore experimentally if there are any “wiggles” in the free energy, which may be associated with some phase changes.

In addition to thermal fluctuations, there are many other sources and types of fluctuations. On the most fundamental level, there are quantum fluctuations, which arise if we measure several non-commuting observables. In heavy-ion collisions, we encounter fluctuations and correlations related to the initial state of the system, fluctuations reflecting the subsequent evolution of the system, and trivial fluctuations induced by the experimental measurement process. Initial state fluctuations are driven by, *e.g.*, inhomogeneities in the initial energy and baryon number deposition. These fluctuations are quite substantial, and are reflected, for example, in higher harmonics of the radial flow field.

In this contribution, we will concentrate on thermal fluctuations, which, away from some phase transitions, are typically small, suppressed by  $1/\sqrt{N}$ , where  $N$  is the average number of particles in the volume considered. We will also be concerned with fluctuations originating in the measurement. These need to be understood, controlled and subtracted in order to access the dynamical fluctuations which tell as about the properties of the system.

In experiment, fluctuations are most effectively studied by measuring so-called event-by-event (E-by-E) fluctuations, where a given observable is measured on an event-by-event basis and its fluctuations are studied for the ensemble of events. Alternatively, one may analyze the appropriate multi-particle correlations measured over the same region in phase space [11].

This contribution is organized as follows. We will first provide a short review on thermal fluctuations and how they can be addressed, *e.g.*, by lattice QCD. We will then discuss various corrections which need to be applied to the data and (model) calculations. We will close with a discussion of the recent preliminary measurement of net-proton cumulants by the STAR Collaboration. Finally, we wish to dedicate this contribution to Andrzej Bialas on the occasion of his 80<sup>th</sup> birthday.

## 2. Fluctuations of a thermal system

The system created in an ultra-relativistic heavy-ion collision reaches, to a very good approximation, thermal equilibrium (see *e.g.* [12] for a recent review). Thermal fluctuations are typically characterized by the appropriate cumulants of the partition function or, equivalently, by equal time correlation functions which, in turn, correspond to the space-like (static) responses of the system. In the following, we will concentrate on cumulants of conserved charges, such as baryon number and electric charge. To this end, we will work within the grand-canonical ensemble, where the system is in contact with an energy and “charge” reservoir. Consequently, the energy and the various charges are only conserved on the average with their mean values being controlled by the temperature and the various chemical potentials. As far as heavy-ion reactions are concerned, the grand-canonical ensemble appears to be a good choice as long as one considers a sufficiently small subsystem of the entire final state. In addition, as discussed *e.g.* in [13], the final-state hadron yields are very well-described by a grand-canonical thermal system of hadrons.

Fluctuations of conserved charges are characterized by the cumulants of susceptibilities of that charge. Given the partition function of the system with conserved charges  $Q_i$

$$Z = \text{Tr} \left[ \exp \left( -\frac{H - \sum_i \mu_i Q_i}{T} \right) \right], \quad (1)$$

the susceptibilities are defined as the derivatives with respect to the appropriate chemical potentials. In the case of three flavor QCD, the conserved charges are the baryon number, strangeness and electric charge,  $(B, S, Q)$ , and we have

$$\chi_{n_B, n_S, n_Q}^{B, S, Q} \equiv \frac{1}{VT^3} \frac{\partial^{n_B}}{\partial \hat{\mu}_B^{n_B}} \frac{\partial^{n_S}}{\partial \hat{\mu}_S^{n_S}} \frac{\partial^{n_Q}}{\partial \hat{\mu}_Q^{n_Q}} \ln Z, \quad (2)$$

where  $\hat{\mu}_i = \mu_i/T$  is the reduced chemical potential for charge  $i$ . Since the pressure is given by  $P = (T/V) \ln(Z)$ , the above susceptibilities also control

its Taylor expansion for small values of the various chemical potentials. For example,

$$\frac{P(T, \mu_B)}{T^4} = \frac{P(T, \mu_B = 0)}{T^4} + \sum_n c_n (\mu_B/T)^n, \quad (3)$$

with the expansion coefficients given by  $c_n = \frac{\chi_n^B}{n!}$ . Such a Taylor expansion is employed in order to determine the QCD equation of state for small chemical potentials [14–16] from lattice QCD, since the fermion sign problem does not allow for a direct calculation. Let us next discuss two examples which illustrate how the study of fluctuations and correlations provide insight into the structure of QCD matter.

### *Net-charge fluctuations*

One example are the fluctuations of the net electric charge. In Refs. [17, 18], it has been realized that the electric charge  $q$  of particles contributes in square to the fluctuations of the net-charge,

$$\langle (\delta Q)^2 \rangle = q^2 \langle (\delta N)^2 \rangle = q^2 \langle N \rangle, \quad (4)$$

where in the last step, we assumed the particles to be uncorrelated. Thus, cumulants of the net-charge are sensitive to the fractional charge of quarks in a quark–gluon plasma. To remove the dependence on the system size, it is convenient to scale the charge variance by another extensive quantity, such as the entropy

$$R = \frac{\langle (\delta Q)^2 \rangle}{S}. \quad (5)$$

A simple estimate using Boltzmann statistics gives [17, 19]

$$R_{\text{QGP}} = \frac{1}{24} \quad (6)$$

for a two-flavor quark–gluon plasma whereas for a gas of massless pions, we obtain

$$R_\pi = \frac{1}{6}. \quad (7)$$

In other words, due to the fractional charges of the quarks and the increased entropy due to the presence of gluons, the charge fluctuations per entropy in a QGP is roughly a factor four smaller than that in a pion gas at the same temperature. In reality, the hadronic phase contains more particles than

pions, and, taking into account hadronic resonances, the charge variance per entropy is reduced by about 30% which leaves about a factor three difference between a hadronic system and a QGP. Also, a system of constituent quarks, without any thermal gluons leads to a ratio of charge fluctuation to entropy similar to a hadron resonance gas [20]. Finally, it is worth pointing out that similar arguments have been utilized to identify the fractional charges in a quantum Hall system as well as the double charge of cooper pairs in measurements of shot noise [21, 22].

Since the above ratio, Eq. (5), contains only well-defined thermal observables, it can be determined using lattice QCD methods, thus accounting for all possible correlations, the presence of strange quarks *etc.* In Fig. 1, we show lattice QCD results for the net-charge variance per entropy based on the calculations for the net-charge variance from [23] and for the entropy density from [24]. We also show the results for a free pion gas and a QGP with three flavors of massless quarks, both using the proper quantum statistics, as well as that for a hadron resonance gas. We see that the hadron resonance gas agrees well with the lattice results for temperatures up to,  $T \lesssim 160$  MeV, which is close to the pseudo-critical or cross-over temperature of  $T_{pc} = 154 \pm 8$  MeV. For temperatures in the range of  $160 \text{ MeV} \lesssim T \lesssim 250 \text{ MeV}$ , the lattice calculations are in between the resonance gas prediction and that of a non-interacting QGP, indicating that some of the correlations leading to resonance formation are still present in

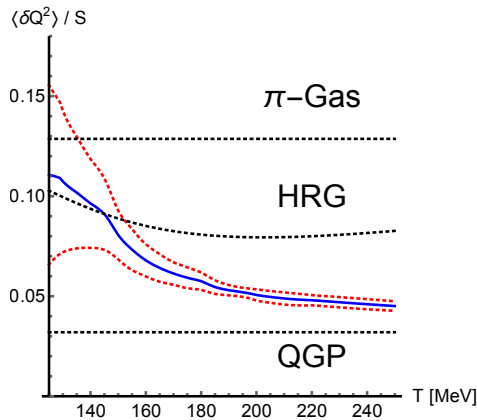


Fig. 1. (Color online) Net-charge variance per entropy,  $R$ , as a function of temperature from 2+1 flavor lattice QCD with physical quark masses. The gray (red) dashed lines indicate the uncertainty. Results for  $\langle (\delta Q)^2 \rangle$  are from [23] and the entropy is extracted from [24]. The dashed horizontal lines indicate the results for a massless pion gas, a hadron gas as well as a non-interacting QGP with three flavors of massless quarks.

the system. With few exceptions, this trend is seen for most quantities which have been calculated on the lattice, such as energy density, cumulant ratios, *etc.* Good agreement with the hadron resonance gas up to the cross-over temperature, followed by a rather smooth transition to a free QGP which takes place over a temperature interval of approximately  $\Delta T \sim 100$  MeV, where the correlations slowly disappear. As we will show in the next example, some of these correlations, namely those between the various quark flavors, can be explored explicitly by studying the so-called mixed flavor or “off-diagonal” cumulants.

### *Correlations between quark flavors*

Let us start by considering the co-variance between strangeness and baryon number,  $\langle \delta B \delta S \rangle \sim \chi_{1,1}^{B,S}$ . To illustrate the sensitivity of this covariance to correlations among quarks, let us again compare a non-interacting QGP with a non-interacting hadron resonance gas (HRG). In the QGP, strangeness is carried exclusively by baryons, namely the strange quarks, whereas in a HRG, strangeness can also reside in strange mesons. Therefore, baryon number and strangeness are more strongly correlated in a QGP than in a hadron gas, at least at low baryon number chemical potential, where mesons dominate. To quantify this observation, Ref. [25] proposed the following quantity

$$C_{BS} \equiv -3 \frac{\langle \delta B \delta S \rangle}{\langle \delta S^2 \rangle} = 1 + \frac{\langle \delta u \delta s \rangle + \langle \delta d \delta s \rangle}{\langle \delta s^2 \rangle}, \quad (8)$$

where we have expressed  $C_{BS}$  also in terms of quark degrees of freedom, noting that the baryon number of a quark is  $1/3$  and the strangeness of a  $s$ -quark is negative one. Here,  $(u, d, s)$  represent the net-number of up, down and strange quarks, *i.e.*, the difference between up and anti-up quarks *etc.* For a non-interacting QGP,  $\langle \delta u \delta s \rangle = \langle \delta d \delta s \rangle = 0$ , so that  $C_{BS} = 1$ . For a gas of kaons and anti-kaons, on the other hand, where a light (up or down) quark is always correlated with a strange anti-quark (kaons) or *vice versa* (anti-kaons)  $\langle \delta u \delta s \rangle < 0$ , resulting in  $C_{BS} < 1$ . Strange baryons, on the other hand, correlate light quarks with strange quarks or light anti-quarks with strange anti-quarks, so that  $\langle \delta u \delta s \rangle > 0$ . Therefore, for sufficiently large values of the baryon number chemical potential,  $C_{BS} > 1$  for a hadron gas, whereas for a non-interacting QGP  $C_{BS} = 1$  for all values of the chemical potential [25]. Since  $C_{BS}$  can be expressed in terms of susceptibilities,  $C_{BS} = -3 \frac{\chi_{11}^{B,S}}{\chi_2^S}$ , it can and has been calculated on the lattice with physical quark masses by two groups [23, 26]. Both calculations agree with each other, and both report a small, but significant difference between the lattice results and that from the hadron resonance gas. In [27], it has been argued that this

discrepancy may be removed by allowing for additional strange hadrons, which are not in the tables of the Particle Data Group (PDG) [28], but are predicted by various quark models. This is shown in Fig. 2, where the lattice QCD results are compared with a hadron resonance gas based on all the hadrons in the Review of Particles [28] (dotted line) and a hadron resonance gas with additional strange hadrons (solid line). Whether or not this turns out to be the correct explanation, this comparison demonstrates that these cumulant ratios are a sensitive probe of the relevant microscopic degrees of freedom.

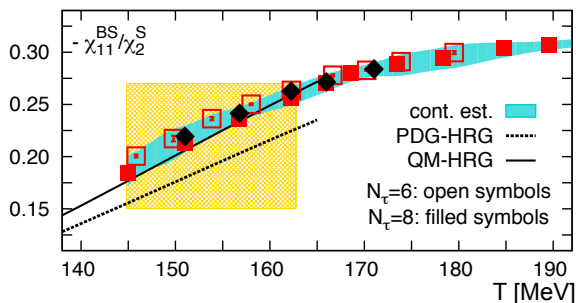


Fig. 2. Lattice QCD results for  $-\frac{\chi_{11}^{B,S}}{\chi_2^S} = \frac{1}{3}C_{BS}$  together with results from hadron resonance gas with and without extra strange mesons. Figure adapted from [27].

To summarize, the above examples illustrate how cumulants of conserved charges can be utilized to extract useful information about the correlations and relevant degrees of freedom of QCD matter. Since they are amenable to lattice QCD methods, the insights derived from such studies are rather model independent.

### 3. Measuring cumulants

#### 3.1. Some general considerations

Given the wealth of information which can be extracted from cumulants of conserved charges and the fact that they can be determined model independently, it would be desirable to measure these cumulants in heavy-ion collisions. However, a heavy-ion collision is a highly dynamical process whereas lattice QCD deals with a static system in global equilibrium. In addition, real experiments have limitations in acceptance *etc.*, which are difficult to map onto a lattice QCD calculation. Consequently, a direct comparison of experiment with lattice QCD results for fluctuation observables is a non-trivial task. In the following, we will discuss various issues which need to be understood and addressed in order for such a comparison to be meaningful.

- **Dynamical evolution:** So far our discussion assumed that the system is static and in global thermal equilibrium. However, even if fluid dynamics is applicable, the system is at best in local thermal equilibrium. The difference between local and global thermal equilibrium is an important aspect of the evolution of fluctuations of conserved charges, because the amount of conserved charge in a given co-moving volume can only change by diffusion, and the rate of diffusion is limited by causality [29]. This observation is central to the use of the variable  $R$  defined in Eq. (5) to detect the presence of quark–gluon plasma. If we consider a sufficiently large rapidity window  $\Delta y$ , then the value of  $R$  is frozen during the QGP phase, and cannot change in the subsequent hadronic stage. Of course, if  $\Delta y$  is chosen too large, then  $R$  never equilibrates, and reflects properties of the initial state. This observation can be made more quantitative using the theory of fluctuating hydrodynamics. However, so far most theoretical studies have focused on schematic models, see, for example, [30].
  
- **Global charge conservation:** Obviously, baryon number, electric charge and strangeness are conserved globally, *i.e.*, if we detected all particles, none of the conserved charges would fluctuate. In contrast, lattice QCD calculations are carried out in the grand-canonical ensemble, which allows for exchange of conserved charges with the heat bath. Consequently, charges are conserved only on the average and, thus, do fluctuate due to the exchange with the heat bath. These exchanges and, thus, the fluctuations depend on the correlations between particles and, as demonstrated above, on the magnitude of the charges of the individual particles. Therefore, in order to compare with lattice QCD, one has to mimic a grand-canonical ensemble in experiment. This can be done by analyzing only a subset of the particles in the final state. However, even in this case, corrections due to global charge conservation are present. These corrections increase with the order of the cumulant [31] and need to be taken into account as discussed in [30, 32–34].
  
- **Finite acceptance:** All real experiments do have a finite acceptance, *i.e.*, they are not able to cover all of phase space. In addition, most experiments are unable to detect neutrons, which do carry baryon number. However, due to rapid isospin exchange processes, the lack of neutron detection may be modeled by a binomial distribution [34]. While it is desirable to study only a subset of particles, in order to mimic a grand-canonical ensemble, it is mandatory to have sufficient coverage in phase space in order to capture all correlations.

- **Efficiency corrections:** A real world experiment detects a given particle only with a probability, commonly referred to as efficiency  $\epsilon$ , which is smaller than one,  $\epsilon < 1$ . However, this does not imply that in every event, the same fraction of produced particles is detected. Rather, the number of measured particles fluctuates even if the number of produced particles does not. In other words, the finite detection efficiency gives rise to fluctuations, which need to be removed or unfolded before comparing with any theoretical calculation. If the efficiency follows a binomial distribution, analytic formulas for the relation between measured and true cumulants can be derived [35–37]. Those have been applied to the most recent analysis by the STAR Collaboration.
- **Dynamical fluctuations:** A heavy-ion collision is a highly dynamical process and the initial conditions as well as the time evolution may easily give rise to additional fluctuations. Especially, at lower energies,  $\sqrt{s} \lesssim 30$  GeV, the incoming nuclei are stopped effectively and deposit baryon number and electric charge in the mid-rapidity region. Clearly, the amount of baryon number deposited will vary from event to event, resulting in fluctuations of the baryon number at mid-rapidity, which are not necessarily the same as those of a thermal system. This potential source of background needs to be understood, especially at low energies where one uses higher cumulants of the net-proton distribution in order to find signals for a possible QCD critical point. Not only does the number of baryon and charges fluctuate due to the collision dynamics, so does the size of the system. And while ratios of cumulants do not depend on the average system size (unless the system is at a second-order phase transition), they are affected by event-by-event fluctuation of the system size. This has been studied in [38] and it was found that only for the very most central collisions, these fluctuations are suppressed. Alternatively, one can devise observables, which are not sensitive to size fluctuation [19, 39–41].

The first three points deserve some additional discussion, as they pose contradictory demands on the measurement [39]. In order to minimize corrections from global charge conservation, one wants to keep the acceptance window  $\Delta$ , say in rapidity, as small as possible. On the other hand, in order to capture the physics, the acceptance window needs to be sufficiently wide in order to catch the correlation among the particles. Therefore, if  $\sigma$  is the correlation length in rapidity and  $\Delta_{\text{charge}}$  the range over which all the charges are distributed, then  $\Delta/\Delta_{\text{charge}} \ll 1$  in order to minimize the effects of charge conservation, and  $\sigma/\Delta \ll 1$  in order to capture the physics.

To illustrate this point, let us consider the following schematic model. Let us define a two-particle correlation function (in rapidity  $y$ )

$$\langle n(y_1) (n(y_2) - \delta(y_1 - y_2)) \rangle = \langle n(y_1) \rangle \langle n(y_2) \rangle (1 + C(y_1, y_2)) \quad (9)$$

with  $\langle n(y) \rangle = \rho = \text{const.}$  Then, the (acceptance dependent) scaled variance of the particle number is given by

$$\frac{\langle (\delta N)^2 \rangle}{\langle N \rangle} = 1 + \frac{\rho}{\Delta} \int_{-\Delta/2}^{\Delta/2} dy_1 dy_2 C(y_1, y_2), \quad (10)$$

where the acceptance in rapidity is given by  $-\Delta/2 < y < \Delta/2$ . Using a simple Gaussian for the correlation function

$$C(y_1, y_2) = \frac{C_0}{\rho} \exp\left(-\frac{(y_1 - y_2)^2}{2\sigma}\right) \quad (11)$$

in Fig. 3, we show the scaled variance as a function of the size of the acceptance window in units of the correlation length  $\Delta/\sigma$ . The solid (black) line is simply the expression of Eq. (10), where we have ignored any effects due to global charge conservation, *i.e.*,  $\Delta_{\text{charge}} \rightarrow \infty$ . The short-dashed (red) and long-dashed (blue) lines represent the situation where the total charge is distributed over a range of  $\Delta_{\text{charge}}/\sigma \leq 5$  and  $\Delta_{\text{charge}}/\sigma \leq 10$ , respectively. Here, we used the leading order formulas of [42] to account for charge conservation, noting that a more sophisticated treatment *à la* [43] would not

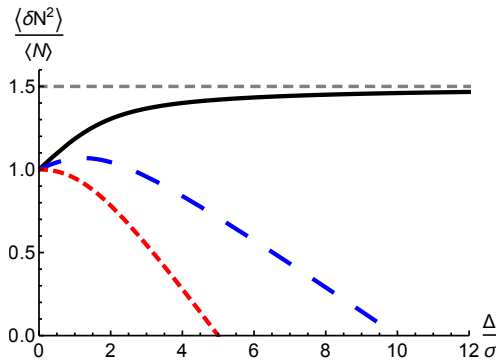


Fig. 3. (Color online) Observed scaled variance as a function of the acceptance window in units of the correlation length. The solid (black) line corresponds to an infinite system where global charge conservation can be ignored. The long-dashed (blue) and short-dashed (red) lines correspond to the situation where the charge is conserved within  $(-10\sigma, 10\sigma)$  and  $(-5\sigma, 5\sigma)$ , respectively.

change the picture qualitatively. Lattice QCD and model calculations, on the other hand, would give the asymptotic value indicated by the horizontal dashed (gray) line, which we have chosen to be  $\frac{\langle(\delta N)^2\rangle}{\langle N\rangle} = 1.5$ . The obvious lesson from this exercise is that a comparison of a measurement at one single acceptance window  $\Delta$  with any model calculation is rather meaningless. Instead, one needs to measure the cumulants for various values of  $\Delta$ , and remove the effect of charge conservation. If the subsequent results trend towards an asymptotic value for large  $\Delta$ , it is this value which should be compared with model and lattice calculations. Such a program has been carried by the ALICE Collaboration in order to extract the aforementioned charge fluctuations [44]. In this context, it is worth mentioning that recent comparisons of measured cumulant ratios with lattice QCD to extract the freeze-out conditions [45, 46] are based on measured cumulants which have not been extrapolated as described above. Thus, these results need to be taken with some care.

Before we turn to the proton cumulants, let us make a few additional remarks concerning efficiency corrections, as they do play a significant role in the recent STAR data [47]. As can be seen in the left panel of Fig. 4, finite detection efficiency,  $\epsilon < 1$ , affects the observed cumulants considerably, and, thus, needs to be corrected or unfolded. As discussed in Refs. [35–37], such an unfolding can be done analytically if the probability for detection of a particle follows a binomial distribution. However, there is no *a priori* reason why the response of a complicated detector should follow a binomial distri-

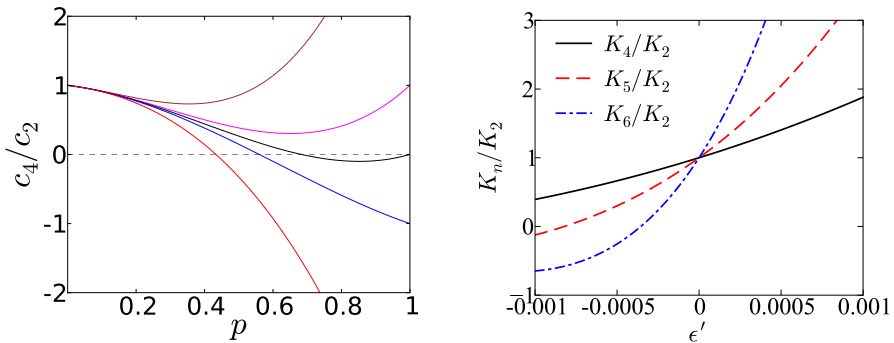


Fig. 4. Left panel: Observed cumulant ratio as a function of binomial probability  $p$ . The lines from top to bottom correspond to true cumulant ratios of  $K_4/K_2 = 5, 1, 0, -1, -5$ . Figure adapted from [35]. Right panel: Effect of multiplicity-dependent efficiency on various cumulant ratios. Deviations from  $K_n/K_2 = 1$  indicate the effect of unfolding based on the binomial distribution with constant efficiency,  $\epsilon_0$ . For reference, the STAR data at 7.7 GeV exhibit a multiplicity dependence corresponding to  $\epsilon' \simeq -5 \times 10^{-4}$  [47]. Figure adapted from [48].

bution. For example, in most experiments, the efficiency depends on the particle multiplicity, which would not be the case for a binomial distribution where the binomial probability, *i.e.*, the efficiency, is constant, independent of the number of Bernoulli trials. In Ref. [48], the effect of a multiplicity-dependent efficiency and various other corrections have been explored. In the right panel of Fig. 4, we show the resulting cumulant ratios  $K_n/K_2$  assuming that the efficiency depends linearly on the multiplicity  $M$

$$\epsilon(M) = \epsilon_0 + \epsilon'(M - \langle M \rangle) .$$

Already a rather weak multiplicity dependence gives rise to correction of the order of 50% for  $K_4/K_2$ .

The multiplicity dependence of the efficiency is just one example for a non-binomial behavior of the detection probability. There are certainly others and some examples are discussed in [48]. Therefore, the only way to assure that detector effects are probably accounted for is for individual experiments to simulate and understand the response of the detector and carry out the necessary unfolding. That such an exercise is necessary should be obvious from the above examples.

### 3.2. Proton cumulants

Let us next turn to the net-proton cumulants. It has been suggested that higher order baryon-number cumulants are particularly sensitive to the presence of a critical point in the QCD phase-diagram [49]. Since it is difficult to detect neutrons, this led to a series of measurements of net-proton cumulants at various energies [47, 50]. As shown in [34], given rapid, pion-driven, isospin exchange, the absence of neutrons can be rather reliably modeled by a binomial process, with binomial probability  $p \simeq 0.5$ . This, on the other hand, implies that in addition to the detection efficiencies, one also needs to unfold the absence of neutrons, or, in other words, detection of protons with an efficiency of 0.8 corresponds to detection of baryons with an effective efficiency of 0.4. As a result, the sensitivity to the correct magnitude of the true cumulants gets considerably reduced as can be seen in the left panel of Fig. 4.

Finally, let us discuss the preliminary results for the  $K_4/K_2$  cumulant ratio for net-protons obtained by the STAR Collaboration. In Fig. 5, we show both the dependence on the beam energy (left panel) and on the width of the rapidity window (right panel) for the lowest beam energy of  $\sqrt{s_{NN}} = 7.7$  GeV. Also shown in the left panel are results from UrQMD calculations. These exhibit a decreasing cumulant ratio with decreasing beam energy, which is due to baryon number conservation [31]. This behavior is in stark contrast with the measured cumulant ratio, which shows a steep

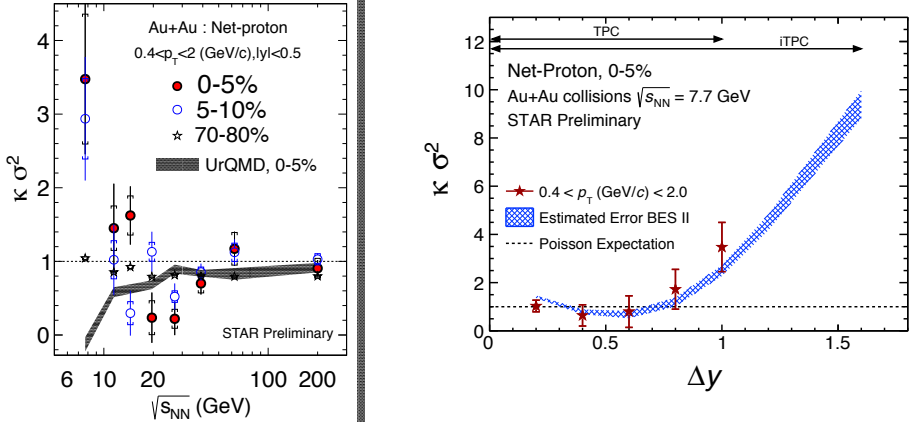


Fig. 5. Preliminary data by the STAR Collaboration for the energy and rapidity dependence of the  $K_4/K_2$  cumulant ratio. Figures adapted from [47, 51].

rise towards lower energies. It is noteworthy that this rise only occurs *after* corrections for efficiency based on a binomial efficiency distribution have been applied [47]. Obviously, these preliminary data are very intriguing, especially since most “trivial” effects tend to reduce the cumulant ratios, such as the aforementioned baryon number conservation. However, in light of our discussion, it will be important that the validity of the binomial efficiency distribution is verified by a detailed analysis of the STAR detector response.

The dependence on the size of the rapidity window, shown in the right panel of Fig. 5, is also quite interesting. The cumulant ratio keeps increasing up to the maximum available range of  $\Delta y = 1$ . Following our simple model consideration, this implies that the underlying rapidity correlations are rather long range. Typically long-range rapidity correlations are associated with early times in the collision. Although this correspondence is somewhat washed out at lower beam energies, it raises the question if the observed signal may be due to some initial state effects such as impact parameter/volume or stopping fluctuations.

#### 4. Discussion

In this contribution, we have discussed fluctuations of conserved charges and their utility for the exploration of QCD matter. In particular, we have concentrated on various cumulants which have the advantage of being accessible to lattice QCD calculations. Alternatively, one may study the underlying correlations, as suggested by Bialas *et al.* [11]. These may actually provide more physical insight into the dynamics at play. If only one particle species is being considered, such as *e.g.* protons, one can relate the cumu-

lants and the correlation functions [52, 53]. For example, the two-particle correlation function is simply given by the first- and second-order cumulants,  $K_1, K_2$ ,

$$C_2 = K_2 - K_1 .$$

However, once net-protons, *i.e.* protons *and* anti-protons, are being considered, no direct relations between the correlation functions and the cumulants exist. Instead, additional (factorial) moments are required, which can be measured but not be calculated in lattice QCD.

To conclude, fluctuations are a powerful tool to explore the structure of QCD matter. They provide insight into the relevant degrees of freedom, their correlations, and possible phase structures. The measurement of fluctuations requires some care. First, the detector response needs to be well-understood and removed by a proper unfolding procedure. Furthermore, since a heavy-ion collision is a highly dynamical process, fluctuations induced by the initial state or by the dynamical evolution need to be understood before a comparison with model or lattice QCD calculations is possible. Preliminary data on net-proton cumulants from the STAR Collaboration show intriguing features, especially at the lowest energies. To which extend they constitute our first glimpse at structures in the QCD phase diagram can only be found out if all these uncertainties are fully understood.

This work is supported by the Director, Office of Energy Research, Office of High Energy and Nuclear Physics, Divisions of Nuclear Physics of the U.S. Department of Energy under Contract No. DE-AC02-05CH11231, and by the Polish Ministry of Science and Higher Education (MNiSW), by founding from the Foundation for Polish Science, and by the Polish National Science Centre (Narodowe Centrum Nauki), Grant No. DEC-2014/15/B/ST2/00175 and in part by DEC-2013/09/B/ST2/00497.

## REFERENCES

- [1] H. Fritzsche, M. Gell-Mann, H. Leutwyler, *Phys. Lett. B* **47**, 365 (1973).
- [2] D.J. Gross, F. Wilczek, *Phys. Rev. Lett.* **30**, 1343 (1973).
- [3] H.D. Politzer, *Phys. Rev. Lett.* **30**, 1346 (1973).
- [4] J.C. Collins, M.J. Perry, *Phys. Rev. Lett.* **34**, 1353 (1975).
- [5] N. Cabibbo, G. Parisi, *Phys. Lett. B* **59**, 67 (1975).
- [6] E.V. Shuryak, *Sov. Phys. JETP* **47**, 212 (1978) [*Zh. Eksp. Teor. Fiz.* **74**, 408 (1978)].
- [7] M. Creutz, *Phys. Rev. D* **21**, 2308 (1980).
- [8] M. Creutz, *Phys. Rev. Lett.* **43**, 553 (1979) [*Erratum ibid.* **43**, 890 (1979)].

- [9] Y. Aoki *et al.*, *Nature* **443**, 675 (2006) [arXiv:hep-lat/0611014].
- [10] M.A. Stephanov, *Prog. Theor. Phys. Suppl.* **153**, 139 (2004) [arXiv:hep-ph/0402115].
- [11] A. Bialas, V. Koch, *Phys. Lett. B* **456**, 1 (1999) [arXiv:nucl-th/9902063].
- [12] P. Braun-Munzinger, V. Koch, T. Schäfer, J. Stachel, *Phys. Rep.* **621**, 76 (2016) [arXiv:1510.00442 [[nucl-th]].
- [13] A. Andronic, *Int. J. Mod. Phys. A* **29**, 1430047 (2014) [arXiv:1407.5003 [nucl-ex]].
- [14] C. Allton *et al.*, *Phys. Rev. D* **66**, 074507 (2002) [arXiv:hep-lat/0204010].
- [15] R.V. Gavai, S. Gupta, *Phys. Rev. D* **78**, 114503 (2008) [arXiv:0806.2233 [hep-lat]].
- [16] S. Borsanyi *et al.*, *J. High. Energy Phys.* **1208**, 053 (2012) [arXiv:1204.6710 [hep-la]].
- [17] S. Jeon, V. Koch, *Phys. Rev. Lett.* **85**, 2076 (2000) [arXiv:hep-ph/0003168].
- [18] M. Asakawa, U.W. Heinz, B. Müller, *Phys. Rev. Lett.* **85**, 2072 (2000) [arXiv:hep-ph/0003169].
- [19] S. Jeon, V. Koch, arXiv:hep-ph/0304012.
- [20] A. Bialas, *Phys. Lett. B* **532**, 249 (2002) [arXiv:hep-ph/0203047].
- [21] L. Saminadayar, D.C. Glatzli, Y. Jin, B. Etienne, *Phys. Rev. Lett.* **79**, 2526 (1997).
- [22] X. Jehl, M. Sanquer, R. Calemczuk, D. Mailly, *Nature* **405**, 50 (2000).
- [23] S. Borsanyi *et al.*, *J. High Energy Phys.* **1201**, 138 (2012) [arXiv:1112.4416 [hep-lat]].
- [24] S. Borsanyi *et al.*, *J. High Energy Phys.* **1011**, 077 (2010) [arXiv:1007.2580 [hep-lat]].
- [25] V. Koch, A. Majumder, J. Randrup, *Phys. Rev. Lett.* **95**, 182301 (2005) [arXiv:nucl-th/0505052].
- [26] A. Bazavov *et al.* [HotQCD Collaboration], *Phys. Rev. D* **86**, 034509 (2012) [arXiv:1203.0784 [hep-lat]].
- [27] A. Bazavov *et al.*, *Phys. Rev. Lett.* **113**, 072001 (2014) [arXiv:1404.6511 [hep-lat]].
- [28] K.A. Olive *et al.* [Particle Data Group], *Chin. Phys. C* **38**, 090001 (2014).
- [29] E.V. Shuryak, M.A. Stephanov, *Phys. Rev. C* **63**, 064903 (2001) [arXiv:hep-ph/0010100].
- [30] M. Kitazawa, M. Asakawa, H. Ono, *Phys. Lett. B* **728**, 386 (2014) [arXiv:1307.2978 [nucl-th]].
- [31] A. Bzdak, V. Koch, V. Skokov, *Phys. Rev. C* **87**, 014901 (2013) [arXiv:1203.4529 [hep-ph]].
- [32] V. Koch, M. Bleicher, S. Jeon, *Nucl. Phys. A* **698**, 261 (2002) [arXiv:nucl-th/0103084]; **702**, 291 (2002).

- [33] M.A. Aziz, S. Gavin, *Phys. Rev. C* **70**, 034905 (2004) [arXiv:nuc1-th/0404058].
- [34] M. Kitazawa, M. Asakawa, *Phys. Rev. C* **86**, 024904 (2012) [arXiv:1205.3292 [nucl-th]].
- [35] A. Bzdak, V. Koch, *Phys. Rev. C* **86**, 044904 (2012) [arXiv:1206.4286 [nucl-th]].
- [36] A. Bzdak, V. Koch, *Phys. Rev. C* **91**, 027901 (2015) [arXiv:1312.4574 [nucl-th]].
- [37] X. Luo, *Phys. Rev. C* **91**, 034907 (2015) [arXiv:1410.3914 [physics.data-an]].
- [38] V. Skokov, B. Friman, K. Redlich, *Phys. Rev. C* **88**, 034911 (2013) [arXiv:1205.4756 [hep-ph]].
- [39] V. Koch, *Hadronic Fluctuations and Correlations*, in: *Relativistic Heavy Ion Physics*, R. Stock (Ed.), Springer, Heidelberg 2010, pp. 626–652, Landolt–Boernstein New Series I, v. 23, ISBN: 978-3-642-01538-0, 978-3-642-01539-7 (eBook) [arXiv:0810.2520 [nucl-th]].
- [40] M. Gazdzicki, M. Gorenstein, M. Mackowiak-Pawlowska, *Phys. Rev. C* **88**, 024907 (2013) [arXiv:1303.0871 [nucl-th]].
- [41] E. Sangaline, arXiv:1505.00261 [nucl-th].
- [42] M. Bleicher, S. Jeon, V. Koch, *Phys. Rev. C* **62**, 061902 (2000) [arXiv:hep-ph/0006201].
- [43] M. Sakaida, M. Asakawa, M. Kitazawa, *Phys. Rev. C* **90**, 064911 (2014) [arXiv:1409.6866 [nucl-th]].
- [44] B. Abelev *et al.* [ALICE Collaboration], *Phys. Rev. Lett.* **110**, 152301 (2013) [arXiv:1207.6068 [nucl-ex]].
- [45] F. Karsch, *Central Eur. J. Phys.* **10**, 1234 (2012) [arXiv:1202.4173 [hep-lat]].
- [46] S. Borsanyi *et al.*, *Phys. Rev. Lett.* **111**, 062005 (2013) [arXiv:1305.5161 [hep-lat]].
- [47] X. Luo [STAR Collaboration], *PoS CPOD2014*, 019 (2014) [arXiv:1503.02558 [nucl-ex]].
- [48] A. Bzdak, R. Holzmann, V. Koch, arXiv:1603.09057 [nucl-th].
- [49] M. Stephanov, *Phys. Rev. Lett.* **102**, 032301 (2009) [arXiv:0809.3450 [hep-ph]].
- [50] L. Adamczyk *et al.* [STAR Collaboration], *Phys. Rev. Lett.* **112**, 032302 (2014) [arXiv:1309.5681 [nucl-ex]].
- [51] X. Luo, Exploring the QCD Phase Structure with Beam Energy Scan in Heavy-ion Collisions, in: 25<sup>th</sup> International Conference on Ultra-Relativistic Nucleus–Nucleus Collisions, Quark Matter 2015, Kobe, Japan, September 27–October 3, 2015, [arXiv:1512.09215 [nucl-ex]].
- [52] B. Ling, M.A. Stephanov, *Phys. Rev. C* **93**, 034915 (2016) [arXiv:1512.09125 [nucl-th]].
- [53] A. Bzdak, V. Koch, in preparation.